# Temporal variations in the Earth's gravity field with emphasis on atmospheric effects

Thomas Peters[1], Jürgen Müller[2], Nico Sneeuw[3]

## Abstract

The determination of the Earth's gravity field is the main goal of the dedicated gravity field missions CHAMP, GRACE and GOCE. The gravity field comprises always a static part and a much smaller time-variable one in the order of millimeters to centimeters, if expressed in geoid heights. As the measurements always consist of both parts, one has to separate them to get a highly accurate static field with high resolution. In this paper, we give a short description of the mathematical model of the time variations in the Earth's gravity field. We briefly discuss the spatial and spectral behaviour of the main processes causing the variations. In detail, the atmospheric impact on the gravity field variations is investigated, and its effect on the satellite missions resp. their measurements is shown. Finally the basic relationship between gravity field coefficients and Earth rotation parameters is given.

## 1 Introduction

The Earth's gravity field depends on the mass distribution of the Earth. Therefore, any mass movements in, on or above the Earth produce variations in the gravity field. On the other hand, mass transport will change the Earth's inertia tensor, which affects the Earth rotation described by the conservation of angular momentum. A better knowledge of these variations will provide information about the global changes and dynamic behaviour of the Earth (Chao, 1994).

For almost two decades, the variations have been observed via perturbations in the orbits of geodetic satellites like LAGEOS. Measurements of the positions of these satellites using SLR (Satellite Laser Ranging) led to the determination of secular and seasonal changes in the gravitational field. Since then, a number of studies have investigated the impact of several geophysical phenomena on the gravitational field. Overviews are given by Chao (1994), the NRC report (1997) and Verhagen (2000), more details can be found e.g. in Wahr et al. (1998), Pail et al. (2000), Le Meur and Huybrechts (2001), Johnson et al. (2001) and the references given therein.

The satellite missions CHAMP, GRACE and GOCE are designed to determine the Earth's gravity field to high accuracy and resolution. They provide consistent global observations, where CHAMP and GRACE are able to observe also temporal variations. For GOCE, the time variable parts have to be modeled to avoid systematic couplings into the static part. Therefore it is necessary to investigate time-dependent effects and to identify the contributions of single sources like ocean tides, post-glacial rebound or the mass redistribution in the atmosphere. The observations of the satellites as well as those with SLR or GPS contain the integral sum of all effects. If one is interested in the single sources, one has to separate them, which can be achieved by specific numerical modeling and by using additional data from in situ observations.

## 2 Modeling a time variable gravity field

In this section, the equations relating mass transports and changes in gravity are derived. The time-dependent change in the Newtonian gravitational potential can be expressed as a sum of spherical harmonics

$$\begin{aligned}\Delta V &= \frac{GM}{R}\sum_{n=0}^{\infty}\left(\frac{R}{r}\right)^{n+1}\sum_{m=0}^{n}\bar{P}_{nm}(\cos\theta)\\ &\quad\cdot\left[\Delta\bar{C}_{nm}\cos m\lambda+\Delta\bar{S}_{nm}\sin m\lambda\right]; \quad (1)\end{aligned}$$

where $R$ is the radius of the Earth; $r$, $\theta$ and $\lambda$ are spherical coordinates of an external point (radius, colatitude and longitude) and $\bar{P}_{nm}$ are the normalized associated Legendre functions of degree $n$ and order $m$. The changes in the dimensionless coefficients are given by:

$$\begin{aligned}\left.\begin{matrix}\Delta\bar{C}_{nm}\\ \Delta\bar{S}_{nm}\end{matrix}\right\} &= \frac{1}{2n+1}\cdot\frac{1}{M}\iiint_{\Sigma}\left(\frac{r}{R}\right)^{n}\Delta\rho(r,\theta,\lambda)\\ &\quad\cdot\bar{P}_{nm}(\cos\theta)\left\{\begin{matrix}\cos m\lambda\\ \sin m\lambda\end{matrix}\right\}d\Sigma. \quad (2)\end{aligned}$$

The density redistribution $\Delta\rho$ as well as the other terms are a function of time. The formulae are valid for single epochs.

This algorithm is known as the Eulerian approach. One focuses on individual points in space, e.g. meteorological stations. Volume integrations are performed

[1]Institut für Astronomische und Physikalische Geodäsie; Technische Universität München; peters@bv.tum.de

[2]Institut für Erdmessung; Universität Hannover; mueller@ife.uni-hannover.de

[3]Department of Geomatics Engineering, University of Calgary, Canada; sneeuw@ucalgary.ca

on the deformed body. After Chao (1994), a second approach can be chosen to describe the problem, the so called Lagrangian approach. There, one follows individual mass particles along their paths, e.g. tracking isobars. Both approaches are equivalent up to first order. The right choice of the approach depends on which data of the mass transport are available. This paper will concentrate on the Eulerian approach.

With the assumption, that all mass redistribution happens in a thin layer of thickness $H$ and causes a change in density $\Delta\hat{\rho}(\theta,\lambda)$ near the surface of the Earth only, the total mass of the Earth can be approximated as $M \approx 4/3\pi G\bar{\rho}$ with a constant mean density $\bar{\rho}$. Now the radial part can be separated and integrated:

$$\int_{r=R}^{R+H} \left(\frac{r}{R}\right)^{n+2} dr = \frac{R}{n+3}\left[\left(\frac{R+H}{R}\right)^{n+3} - 1\right] \approx H\left[1 + \frac{(n+2)}{2}\frac{H}{R} + \ldots\right]. \quad (3)$$

The truncation of the expansion into binomial series simplifies the computation and avoids numerical problems ($H \ll R$), but produces small errors increasing with degree $n$. The density $\hat{\rho}$ times the height $H$ is the surface density $\sigma$ of a thin layer. The changes in surface density $\Delta\sigma$ are the radial integration of $\Delta\rho$ over the layer. Equation (2) reduces to:

$$\left.\begin{matrix}\Delta\bar{C}_{nm}\\ \Delta\bar{S}_{nm}\end{matrix}\right\} = \frac{3}{4\pi R\bar{\rho}(2n+1)} \iint_{\sigma} \Delta\sigma(\theta,\lambda) \cdot \bar{P}_{nm}(\cos\theta)\left\{\begin{matrix}\cos m\lambda\\ \sin m\lambda\end{matrix}\right\} d\sigma. \quad (4)$$

This equation describes only the contribution to the gravitational potential from the direct gravitational attraction of the surface mass. But the surface mass also loads and deforms the underlying solid Earth, which causes an additional contribution to the potential, described by the load Love number $k'_n$ of degree $n$, cf. Munk and MacDonald (1960) or Wahr et al. (1998).

The total potential change is the sum of these two contributions:

$$\left.\begin{matrix}\Delta\bar{C}_{nm}\\ \Delta\bar{S}_{nm}\end{matrix}\right\} = \frac{3(1+k'_n)}{4\pi R\bar{\rho}(2n+1)} \iint_{\sigma} \Delta\sigma(\theta,\lambda) \cdot \bar{P}_{nm}(\cos\theta)\left\{\begin{matrix}\cos m\lambda\\ \sin m\lambda\end{matrix}\right\} d\sigma. \quad (5)$$

For the use of existing programs for the computation of eq. (5), $\Delta\sigma$ can be represented in terms of spherical harmonics

$$\Delta\sigma(\theta,\lambda) = R\,\rho_w \sum_{n=0}^{\infty}\sum_{m=0}^{n} \bar{P}_{nm}(\cos\theta) \cdot[\Delta\hat{C}_{nm}\cos m\lambda + \Delta\hat{S}_{nm}\sin m\lambda] \quad (6)$$

with new coefficients $\hat{C}_{nm}$ and $\hat{S}_{nm}$. The factor $R\cdot\rho_w$ (with $\rho_w$ a constant density of water) is introduced in order to get dimensionless new coefficients.

After applying a spherical harmonic analysis to eq. (6), a comparison of the coefficients yields the following simple transfer in the spectral domain:

$$\left.\begin{matrix}\Delta\bar{C}_{nm}\\ \Delta\bar{S}_{nm}\end{matrix}\right\} = \frac{1+k'_n}{2n+1}\cdot\frac{3\rho_w}{\bar{\rho}}\left\{\begin{matrix}\Delta\hat{C}_{nm}\\ \Delta\hat{S}_{nm}\end{matrix}\right\} . \quad (7)$$

Together with (1), this gives the change in the gravitational potential and models any effect caused by the change in the surface density.

The derivation of changes in the surface density from measured data must be treated separately for each physical effect (see e.g. section 4 for the atmospheric effect).

## 3 Sources causing gravitational time variations

First, one has to identify, which mass transport produces significant and measurable geodynamic effects. Chao (1994) gives two criteria: a sufficiently large amount of mass has to be involved and the effective mass transport has to cover great distances. For example, shipping of goods, steric changes in sea level or the formation of polar sea ice are not significant due to the criteria given above.

The NRC report (1997) provides an inventory of the processes causing significant effects. Figure 1 shows their results characterized by the magnitude, periods and the spatial scales (wavelength) of every effect. Tides are not shown here, because they appear at nearly all periods and spatial scales with magnitude up to $10^{-7}g$ (Torge, 2001) with $g$ the mean gravity acceleration. Only the tidal deformation produced by the tidal forces in the solid Earth and in the oceans, but not the direct luni-solar tidal torques affecting the Earth rotation has to be considered. These forces are of interest, when one assumes that the Earth responds to the tidal decelaration by becoming less oblate (Chao, 1994).

The largest effects with seasonal to interannual periods are those of the atmosphere and the hydrosphere, while post-glacial rebound causes the biggest contribution to the secular effects. Here, the secular variations mean those slower than a number of years. We do not consider changes in geological time scales.

The atmospheric mass transport is responsible for gravity variations in the order of approx. $10^{-8}g$. Besides the dominant seasonal signals, also shorter periods and smaller variations may produce large effects (see chapter 4).

Hydrosphere means the distribution of water on land and in the oceans. Mass transport is carried out by

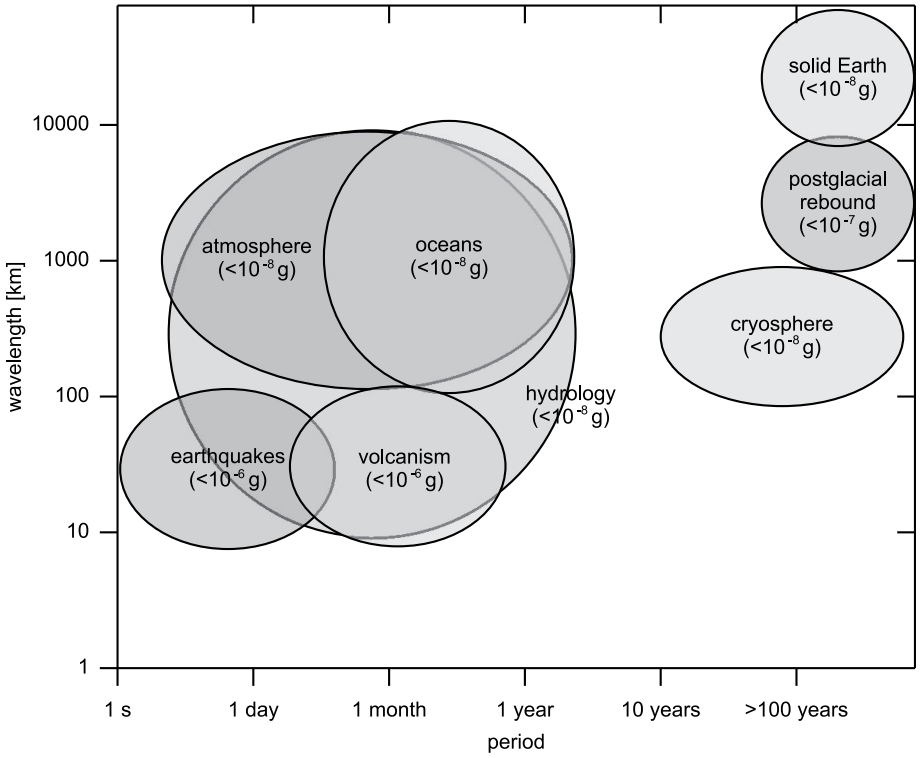


**Figure 1:** Expected periods, wavelengths and magnitude of each geophysical effect (from: Verhagen (2000) after NRC (1997) and Torge (1989)).

the circular flow of water with precipitation, evapotranspiration and runoff. To model these variations, one needs data about snow cover, ground-water, precipitation, soil moisture, new artificial reservoirs and so on for the land area. Unfortunately, some of these parameters are only available with insufficient quality and poor spatial coverage. For the oceans, one needs information about the thermal-haline and wind-driven circulation in the oceans as well as the rise of the sea level, e.g. from satellite altimetry. Recent results for such simulations can be found in Wünsch et al. (2001).

The behaviour of ice sheets has to be seen in conjunction with the sea level rise and the post-glacial rebound. Less is known about the total ice mass balance of Antarctica and Greenland. The effects are probably small, but they are present. Post-glacial rebound after the last ice-age can be modeled quite well for regions like Northern America or Scandinavia, problems occur in presently glaciated areas. The uplift of the mantle reduces the Earth's oblateness and is probably responsible for the secular drift in the polar motion.

Mass redistribution due to volcanism and earthquakes show up with very short periods and spatial expansions and are hardly ever predictable, so one only can assess the results after such events. Moreover, most of them have been too small to have any detectable geodynamic effect. The effects of solid Earth processes like activities of the core or the mantle convection with tectonic movements are not very well understood.

## 4 The effect of the atmosphere

The atmosphere is almost hydrostatic and the mass distribution in the atmosphere is directly related to the atmospheric pressure by the hydrostatic equation:

$$dp = -g\rho\, dh \ . \tag{8}$$

The change in atmospheric mass integrated vertically above a point on the Earth's surface is proportional to the change in atmospheric pressure at this point. Comparing the radial integration over density changes

$$\Delta p(\theta,\lambda) = g \int_r \Delta\rho(r,\theta,\lambda)\, dr \tag{9}$$

with the definition of changes in the surface density $\Delta\sigma$, one finds:

$$\Delta\sigma(\theta,\lambda) = \frac{\Delta p(\theta,\lambda)}{g} \ . \tag{10}$$

Thus, after subtraction of a long-time medium field $\bar{p}(\theta,\lambda)$, global gridded values of atmospheric pressure

can be used to find the changes in the surface densities.

Equation (8) shows the dependency of the atmospheric pressure on the height. Density and pressure are very small at heights of 15 km, so the thin layer assumption seems to be justified when thinking of the altitude of the satellites of about 250–450 km. Nevertheless, this assumption introduces small errors.

While the pressure is decreasing with increasing height, two different kinds of atmospheric pressure data are available: the observed surface pressure and a reduced sea level pressure. For our applications, surface pressures are needed. To estimate the changes in atmospheric mass, 11 years (1990-2000) of daily global pressure fields as well as derived monthly means provided by the NCEP (National Center for Environmental Prediction) reanalysis project of the NOAA-CIRES Climate Diagnostics Center are used (see Kalnay et al., 1996). The data are interpolated to a $2.5° \times 2.5°$ grid and available for free[4]. Using monthly means causes a loss of information, but saves a lot of processing time.

The pressure data are further processed to consider the ocean response to pressure variations nearly like an inverted barometer (IB) response, see (Wunsch and Stammer, 1997), i.e. an increase in atmospheric pressure of 1 hPa should cause the underlying ocean surface to decrease by 1 cm, so that there is no net change in mass integrated vertically through the overlying ocean and atmosphere. Setting $\Delta\sigma = 0$ over the oceans is equivalent to include the redistribution of atmospheric mass over the oceans and of oceanic mass caused by the load of the atmospheric pressure fluctuations in $\Delta\sigma$ (Wahr et al., 1998). In reality, the ocean does not behave exactly like an IB. Some examples of a refined modeling are presented in Verhagen (2000). In the following, the IB assumption is considered mostly. Only figure 2 and 3 include exemplary results for the NIB case, where the pressure variations are taken as they are observed on the Earth's surface.

Now one can set up the computation:

- Subtraction of a long-time mean $\bar{p}$ yields $\Delta p$.
- Eq. (10) gives $\Delta\sigma$.
- Setting $\Delta\sigma = 0$ for ocean areas (use of a land-ocean-mask) takes the IB assumption into account.
- Expand $\Delta\sigma$ into spherical harmonics (eq. (6)).
- Transform into changes in the coefficients $\bar{C}_{nm}$ and $\bar{S}_{nm}$ with eq. (7).
- Derivation of the change in the gravitational potential or its functionals.

[4]Download from `http://www.cdc.noaa.gov/Datasets/ncep.reanalysis.dailyavgs/surface/`

Figure 2 shows atmospheric pressure anomalies $\Delta p$ on January 1, 2000 for the NIB and IB assumption, figure 3 gives the resulting geoid change for the two cases. The amplitudes in both figures can be considered as representative also for other days. The shown geoid effect consists of the direct and the indirect effect, where the direct effect exceeds the indirect one by about five to ten times. In general, the NIB assumption results in larger values, but the IB assumption is closer to reality.

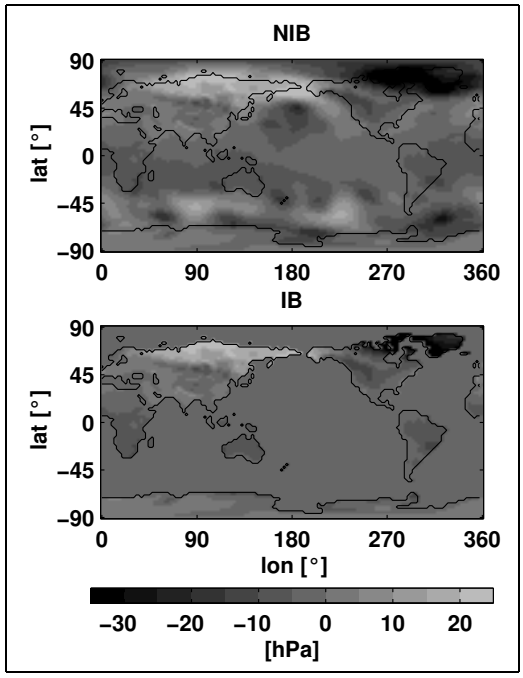


**Figure 2:** $\Delta p$ on January 1, 2000

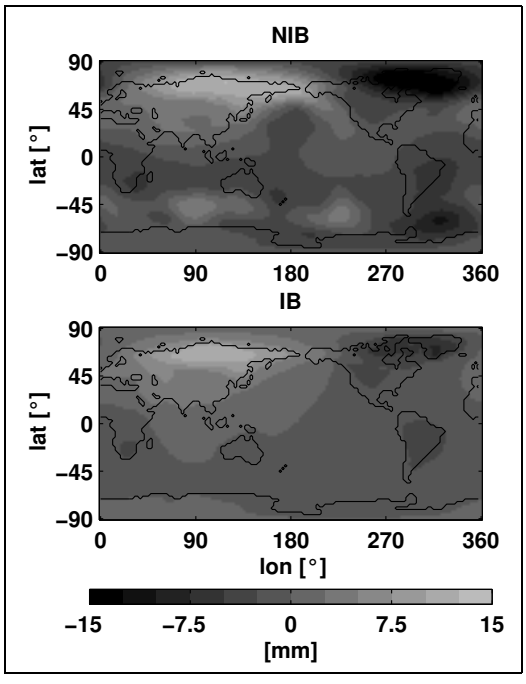


**Figure 3:** Total geoid effect on January 1, 2000

The time series of atmospheric pressure variations or those of the resulting geoid changes, both under the IB assumption, show a different spectral behaviour and amplitudes for nearly every place on Earth. Therefore, a simplification like the computation of a worldwide mean value does not make any sense for the analysis of gravity variations. One has to take worldwide pressure variations into account. A useful term for the analysis are the degree variances of the potential coefficients. Their rms-value $\mathrm{RMS}_n$ represents an average value of the single coefficients per degree and is given by

$$\mathrm{RMS}_n = \sqrt{\frac{1}{2n+1}\sum_{m=0}^{n}(\Delta\bar{C}_{nm}^2 + \Delta\bar{S}_{nm}^2)}\ . \qquad (11)$$

A time series from 1990 to 2000 of monthly mean potential coefficients in eq. (11) yields the upper field shown in figure 4. Their Fourier-transform is given in the lower panel of figure 4. Here, a dominant annual period and a significant semi-annual period can be identified. In comparison to them, all lower and higher frequencies up to a two-daily one are small, but the sum of all the other frequencies is still powerful and cannot be neglected without loss of important information. Furthermore, one has to be aware of problems with aliasing and leakage.

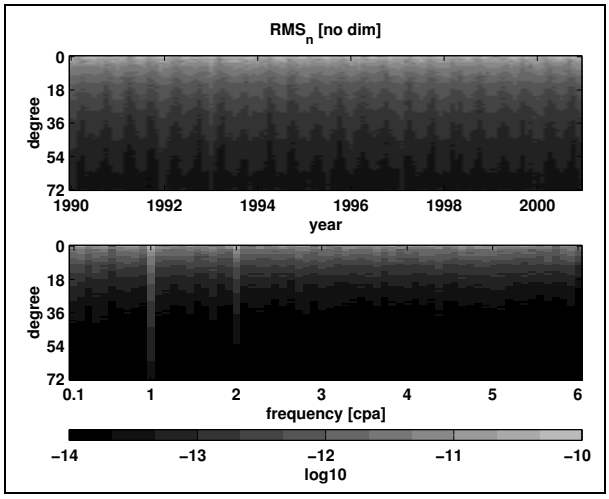


**Figure 4:** Degree RMS of 11 years monthly means

The spatial distribution of the amplitudes of the two main frequencies are shown in figure 5. A significant bulls-eye over central Asia of about 6 mm geoid height contribution is visible, while the semi-annual period has its maximum with nearly 3 mm over Antarctica.

These results agree quite well with those of other studies from Wahr et al. (1998), Pail et al. (2000) or Verhagen (2000).

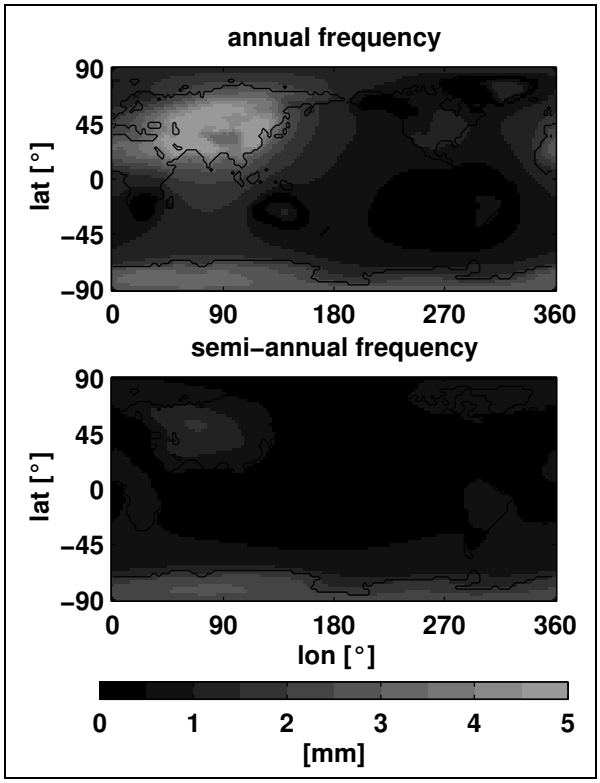


**Figure 5:** Amplitudes in geoid height variation $\Delta N$ for the dominant frequencies

## 5 Effect on satellite missions

The effect of the gravity variations on satellite missions like GRACE and GOCE is of special interest and was the main reason to set up this study. One has to compare the measurement accuracy of the satellite sensors with the signal power of the time-variable effects. This can be done by using the degree-rms of eq. (11) of the gravity variations and the expected degree-rms of the satellite missions. Figure 6 shows the degree-rms of the two main frequencies of the atmospheric effect from figure 4 and those of GRACE and GOCE.

The signal of the annual period is about 3–5 times higher than that one of the semi-annual period. Theoretically, the measurement of the effect is possible while the atmospheric signal exceeds the measurement accuracy, which holds up to degree 15 for GOCE and up to degree 32 for GRACE. All other frequencies are less and will hardly be measurable. In fact, semi-annual and annual signals cannot be observed by GOCE because the mission duration is only two times 6 months. But the temporal signals have to be removed from the GOCE data, not to cause systematic errors when determining the static part of the gravity field. With GRACE, temporal signals down to monthly periods can be resolved.

It should be noted that the point of intersection of the graphs strongly depends on assumptions about

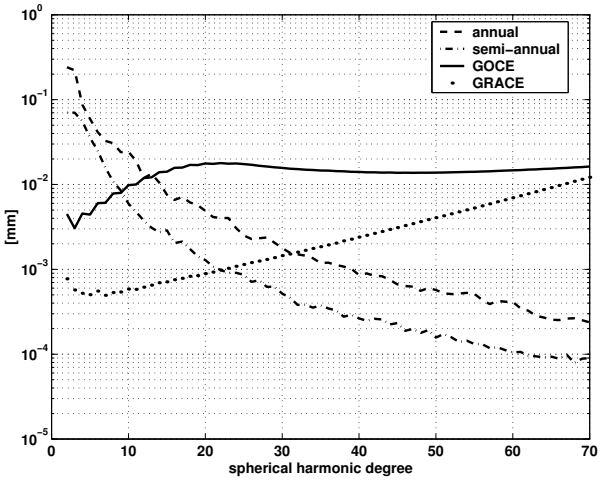


**Figure 6:** $\mathrm{RMS}_n$ of the atmospheric effect, from GRACE and GOCE

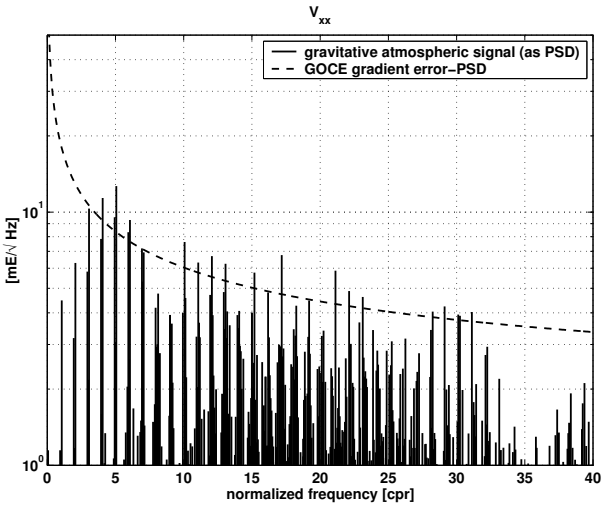


**Figure 7:** Along-track component

the measurement accuracy of the satellites and on the spatial and temporal resolution of the atmospheric pressure data. Also modeling specifications like the IB assumption have an impact on the results.

The impact on the measurements of GOCE can also be estimated by computing the second radial derivate of the effect in the gravitational potential. For a direct comparison with GOCE gradients, a transformation into a satellite fixed coordinate system has to be performed. First, the changes in the gravitational potential are expressed depending on the Keplerian orbit elements of the satellite. Then, one can expand the potential into a 2D-Fourier series with new coefficients, so-called lumped coefficients, at a nominal orbit, i.e. a circular orbit with constant inclination, which is secularly precessing due to the Earth's oblateness, cf. (Sneeuw, 2000). Mapping of this two-dimensional signal to the one-dimensional orbit and multiplication of the lumped coefficients with the root of the mission length yields the atmospheric signal as a PSD in the satellite system.

Figures 7–9 show an example of this approach for the three spatial components. The atmospheric signal of a single day is compared to a simplified GOCE-scenario with a sun-synchronous circular orbit at an altitude of 250 km and a mission length of 3 months. The along-track and particularly the cross-track signal are less.

Although this example is simplified, simulated and maybe not representative, it shows the tendency of the influence of the atmospheric effect on the satellites measurements. The accelerometers will be influenced noticeable in along-track and radial direction, while the cross-track component stays almost unchanged. Therefore parts of the atmospheric effect will be sensed in along-track and radial direction, but not in the cross-track direction.

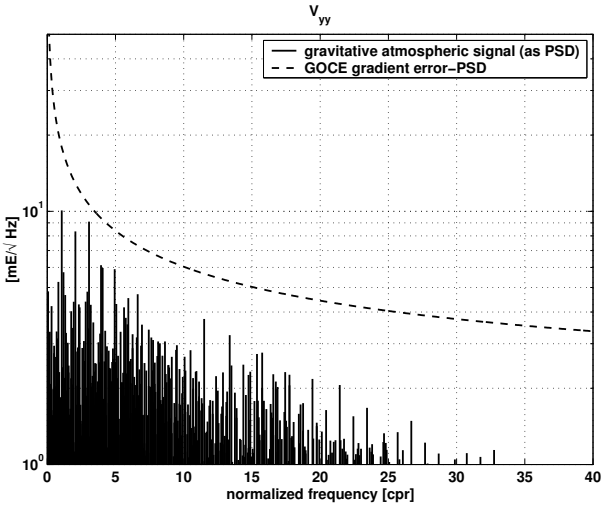


**Figure 8:** Cross-track component

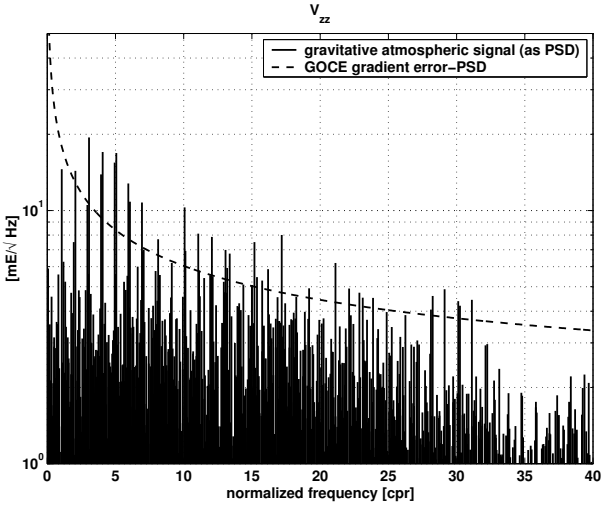


**Figure 9:** Radial component

## 6 Gravity variations and Earth's rotation

To get a more global understanding of physical processes, it is necessary to consider also other geodetic meaurements, which are affected by mass movements. Besides the gravity field coefficients and observables at satellite altitude, Earth's rotation parameters are of special interest. The temporal variations in the gravity field allow the investigation of changes in the Earth's rotation. Vice-versa the investigation of Earth orientation parameters (EOP) indicates mass movements in and on the Earth. Therefore a common analysis of gravity parameters and EOPs may help to better understand the physical processes, which cause these signals. The relationship between gravity and EOPs is briefly discussed here. More details on this topic can be found, e.g., in Chao and Gross (1987), Gross (1992 and 2001) or Gegout and Cazenave (1993) and the references therein. On the one hand, the changing distribution of mass causes the Earth's gravitational field to change (as discussed above). On the other hand, mass movements will also cause the Earth's angular momentum to change, i.e. the Earth's rotation changes in its amplitude and its direction. By measuring the variations in the second-degree spherical harmonic coefficients, which are related to the elements of the Earth's inertia tensor, CHAMP and GRACE will directly observe changes in the Earth's rotation caused by mass redistribution.

The relationship between the variations of the second-degree spherical harmonics and those of the components of the inertia tensor $\Delta I_{ij}$ is given by (cf. Chao and Gross, 1987):

$$\Delta C_{21} = -\frac{\Delta I_{xz}}{MR^2} \quad (12)$$

$$\Delta S_{21} = -\frac{\Delta I_{yz}}{MR^2} \quad (13)$$

$$\Delta S_{22} = -\frac{\Delta I_{xy}}{2MR^2} \quad (14)$$

$$\Delta C_{20} = -\frac{3\Delta I_{zz} - Tr(\Delta I)}{2MR^2} \quad (15)$$

$$\Delta C_{22} = \frac{\Delta I_{yy} - \Delta I_{xx}}{4MR^2} \quad (16)$$

where $M$, $R$ indicate the mass and the radius of the Earth and $Tr(\Delta I)$ the trace of the inertia tensor. The symmetric inertia tensor has six independent elements, whereas there are only five independent second-degree coefficients. That means, the inversion of the formulas above is only possible if special assumptions about the trace are made.

According to the principle of conservation of angular momentum, the rotation of the Earth will change, if the inertia tensor of the Earth changes. An analytical description of polar motion and variations in the length of day (lod) can be achieved with the help of so-called excitation functions $\chi$ which in turn depend on the moments of inertia. In a very simple formulation one has (see e.g. Wahr, 1982):

$$\frac{\dot{m}}{\sigma_0} + m = \chi \quad (17)$$

$$\dot{m_z} = \dot{\chi}_z \quad (18)$$

with the frequency of the Chandler wobble $\sigma_0$, the complex description of polar motion $m = m_x - im_y$ in $x$- and $y$-direction and changes in lod $m_z$. The excitation functions are given by:

$$\chi = \frac{1.61}{\Omega(I_{zz} - I_{xx})}(\Omega\Delta I_c - \Delta h) \quad (19)$$

$$\chi_z = -\frac{\Delta I_{zz}}{I_{zz}} + \frac{\Delta h_z}{\Omega I_{zz}} \quad (20)$$

with the mean rotation rate of the Earth $\Omega$, the variation of the relative angular momentum $\Delta h$ and the complex-valued moment of inertia $\Delta I_c = \Delta I_{xz} - i\Delta I_{yz}$. $I_{xx}$ and $I_{zz}$ are the (unperturbed) equatorial and polar principal moments of inertia. The factor 1.61 accounts for the decoupling of the core and the mantle. Under a further simplification (i.e. neglecting the relative angular momentum which represents the so-called motion terms), the excitation functions may be written

$$\chi = \frac{1.61\Delta I_c}{\Omega(I_{zz} - I_{xx})} \quad (21)$$

$$\chi_z = -\frac{\Delta I_{zz}}{I_{zz}} \quad (22)$$

These final equations describe only the mass terms in the excitation functions. The mass terms are of special interest because they depend on the same source mechanisms that change the geoid, while the motion terms, which are important for the investigation of Earth's rotation, do not affect the geoid. Using equations (12)-(16), the direct relation between EOP and the second-degree spherical harmonic coefficients is achieved.

## 7 Discussion

Mass redistribution causes changes in the Earth's gravity field and in the Earth's rotation. In this paper the effect of atmospheric mass movements was investigated in detail. The results show two dominant frequencies — annual and semi-annual — with amplitudes up to 6 mm in terms of geoid height change. This signal will be clearly measurable by GRACE. Since GRACE measures a combination of all time-variable effects, though, the critical question is, whether the atmospheric effects can be distinguished from others. If one wants to learn something about the other time-variable effects, especially the smaller ones, the atmospheric part should be modeled carefully. Velicogna et al. (2001) studied this topic and achieved some promising results.

As was demonstrated, the atmospheric signal will also be perceivable by GOCE. Due to GOCE's shorter mission duration, however, it is considered as noise. A further complication is the fact that the two measurement periods of GOCE have a large seasonal overlap. The time-variable effects, especially those at the annual frequency, will alias into the GOCE gravity field. Therefore the atmospheric signal needs to be corrected for by proper modeling. For this, surface pressure data is needed with high spatial and temporal resolution.

Mass changes are also visible in time series of Earth Orientation Parameters. A combined analysis of EOP and gravity data will be helpful therefore to investigate mass changes caused by processes of the core, the mantle or the crust as well as those by oceanic, atmospheric or tidal effects. Here, we briefly described the fundamental relationship between variations in the second degree spherical harmonics and those of the components of the inertia tensor, which again affect Earth's rotation.

In a next step, aliasing with orbit frequencies need to be considered as well as the backward computation with simulated or real data (e.g. from CHAMP or GRACE). Also the other geophysical phenomena as described above have to be investigated in this way.

## References

Chao B.F. (1994): The Geoid and Earth rotation, in: Vaníček P., N.T. Christou: *Geoid and its geophysical interpretations*, CRC Press, Boca Raton

Chao B.F., R.S. Gross (1987): Changes in the Earth's rotation and low-degree gravitational field induced by earthquakes, *Geophys. Journ. R. astr. Soc.*, **91**:569–596

Gegout P., A. Cazenave (1993): Temporal variations of the Earth's gravity field for 1985–1989 derived from LAGEOS I, *Geophys. Journ. Int.*, **114**:347–359

Gross R.S. (1992): Correspondence between theory and observations of polar motion, *Geophys. Journ. Int.*, **109**:162–170

Gross R.S. (2001): Gravity, oceanic angular momentum, and the Earth's rotation, in: *Proceedings of GGG2000*, in press

Johnson T.J., C.R. Wilson, B.F. Chao (2001): Nontidal oceanic contributions to gravitational field changes: Predictions of the Parallel Ocean Climate Model, *Journ. Geophys. Res.*, **106**(B6):11,315–11,334

Kalnay E., et al. (1996): The NCEP/NCAR 40-year reanalysis project, *Bull. Am. Meteorol. Soc.*, **77**:437–471

Le Meur E., P. Huybrechts (2001): A model computation of the temporal changes of surface gravity and geoidal signal induced by the evolving Greenland ice sheet, *Geophys. Journ. Int.*, **145**:835–849

Munk W.H., G.J.F. MacDonald (1960): *The rotation of the Earth*, Cambridge University Press

NRC (1997): *Satellite gravity and the geosphere*, National Academic Press, Washington

Pail R., H. Sünkel, W. Hausleitner, E. Höck, G. Plank (2000): Temporal variations / Oceans, in: *From Eötvös to mGal*, Draft final report, ESA, Graz

Sneeuw N. (2000): *A semi-analytical approach to gravity field analysis from satellite observations*, Deutsche Geodätische Kommission, Reihe C, Heft 527

Torge W. (1989): *Gravimetry*, de Gruyter, Berlin

Torge W. (2001): *Geodesy*, de Gruyter, Berlin

Velicogna I., J. Wahr, H. van den Dool (2001): Can surface pressure be used to remove atmospheric contributions from GRACE data with sufficient accuracy to recover hydrological signals? *Journ. Geophys. Res.* **106**(B8):16,415–16,434

Verhagen S. (2000): *Time variations in the gravity field — the effect of the atmosphere*, diploma thesis at TU Delft (unreleased)

Wahr J., (1982): The effects of the atmosphere and oceans on the Earth's wobbles — Theory, *Geophys. Journ. R. astr. Soc.* **70**:349–372

Wahr J., F. Bryan, M. Molenaar (1998): Time variability of the Earth's gravity field: Hydrological and oceanic effects and their possible detection using GRACE, *Journ. Geophys. Res.* **103**(B12):30,205–30,229

Wünsch J., M. Thomas, T. Gruber (2001): Simulation of oceanic bottom pressure for gravity space missions, *Geophys. Journ. Int.* **147**:428–434

Wunsch C., D. Stammer (1997): Atmospheric loading and the oceanic "inverted barometer" effect, *Rev. Geophys.* **35**(1):79–107